

Microstructure evolution of spray-formed hypereutectic Al–Si alloys in semisolid reheating process

Xue-wei ZHU, Ri-chu WANG, Jian PENG, Chao-qun PENG

School of Materials Science and Engineering, Central South University, Changsha 410083, China

Received 29 July 2013; accepted 21 November 2013

Abstract: The Al–27%Si alloy was prepared by the spray forming process, and its microstructure evolution during the semisolid reheating process was investigated. The results show that, the primary Si phase coarsens during the reheating process and the coarsening rate increases with the increase of reheating temperature. The eutectic phase is produced in the molten region when quenched in the cold water. The microstructure evolution in the semisolid state can be divided into three stages. The remarkable characteristic of the first stage is only a solid-state phase transformation process. However, the region around the $\alpha(\text{Al})$ matrix gradually melts in the second stage. The primary Si in the liquid phase coarsens obviously, and the eutectic phase is produced in the molten region when the specimens are quenched in cold water. In the last stage, the same thing as that in the second stage happens except that all the $\alpha(\text{Al})$ matrixes are melted.

Key words: spray forming; Al–Si alloy; semisolid; coarsening rate

1 Introduction

Spray forming is a relatively new metallurgical process for manufacturing near net shaped metallic products with enhanced material properties and performance due to the unique microstructure. Liquid metals are atomized into small droplets by the inert gas and deposited on a substrate to form a billet. During the process, liquid metals are solidified with high cooling rates in the range of 10^2 – 10^3 °C/s and fine equiaxed-grained microstructures are obtained. Hypereutectic Al–Si alloys are versatile materials. Al–Si alloys are attractive candidate materials for aerospace, automotive and electronics applications due to their excellent properties, such as low coefficient of thermal expansion, low density, high stiffness and good wear resistance. Because of the solution ability of the silicon and aluminum, the Al–Si alloys can be recycled [1,2].

The microstructures of spray-formed Al–Si alloys show a uniform distribution of Si particles in the Al matrix, especially in hypereutectic Al–Si alloys [3–5]. However, due to the gas and many complex process parameters, porosity is one of the important but undesirable characteristic of the spray-formed

materials [6]. Thus, the spray-formed materials always need a densification process before application. Conventional forming methods [7,8], such as extrusion and roll, were used to densify the spray-formed materials. However, the plastic deformation of Al–Si alloys becomes difficult with the increase of Si content, because a large number of non-deformable Si particles restrict the movement of dislocation [9].

Recently, semisolid forming process is associated with the spray-formed materials [10–14]. Semisolid forming is recognized as a technology which offers several potential advantages over casting and forging, such as reduction of macro-segregations and porosity. Compared with conventional forming methods, semisolid forming can easily accomplish what conventional forming can, but requires lower deformation load due to its low deformation resistance, and consequently, it enables a decrease in energy and machining costs.

It is well known that spray-formed materials have a unique microstructure which is called non-equilibrium state microstructure. However, during the semisolid reheating process, solid phase and liquid matrix coexist. The solid phase in the liquid matrix coarsens rapidly, which may affect the final microstructures and

mechanical properties significantly and the non-equilibrium microstructure has a trend to transform into equilibrium microstructure gradually. Therefore, knowledge of the microstructure evolution of the hypereutectic Al–Si in the semisolid process is essential for the application of spray forming Al–Si alloy. In the present work, Al–27%Si alloy was prepared by the spray forming process, and the mechanism of the microstructure evolution in semisolid state was investigated.

2 Experimental

Spray forming process was employed to prepare Al–27%Si composite. Pure Al with a purity of 99.995%, and crystal silicon were used as the raw materials to minimize the effect of impurity on properties. The molten metal with a superheat of 100 K was atomized by a scanning atomizer. Nitrogen was used as the atomize gas with a pressure of 0.6 MPa. The diameter of the pouring nozzle for melts was 3.5 mm. The cylindrical billet was deposited on a rotating steel substrate with a diameter of 400 mm. The spray distance was 300 mm. The withdraw speed of substrate was adjusted during the spray forming process to keep the spray distance constant. Figure 1 shows the schematic drawing of the spray forming apparatus used in this work.

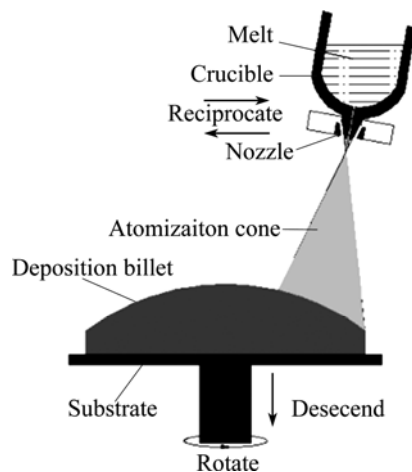


Fig. 1 Schematic drawing of spray forming apparatus used in this work

The specimens were cut with dimensions of 10 mm × 10 mm × 10 mm. Specimens were reheated in a resistance furnace at 590, 600 and 610 °C for 4, 8, 10, 12, 14, 16, 30, and 60 min, respectively, and then quenched in cold water (Firstly, the specimens were put on an Al₂O₃ ceramic substrate and heated at 570 °C for 3 min, and then heated up to the experiment temperature with a heating rate of 10 °C/min.). The microstructures were analyzed by a scanning electron microscope (SEM,

Japan field emission Sirion 200) with an energy-dispersive X-ray (EDX) detector and POLYVAR-MET wide view metallographic microscope.

3 Results and discussion

3.1 Microstructure analysis

Figure 2 shows the SEM images of Al–27%Si alloy prepared by the casting and the spray forming processes, respectively. The microstructure of the as-cast Al–27%Si alloy is mainly composed of primary Si phase and needle-like eutectic Al–Si phase, as shown in Fig. 2(a). The primary Si phase has sharp edges and distributes non-uniformly in the as-cast alloy. Figure 2(b) shows the microstructure of the as-spray formed alloy, which is composed only of the fine Si particles and the α (Al) matrix. The Si particles in the as-spray formed alloy were distributed uniformly, and the needle-like eutectic phases, which were observed in the as-cast alloy, were not found. The size of the primary Si phase in the as-spray formed alloy is less than 5 μ m, which is over 100 μ m in the as-cast alloy. The difference of microstructures of the as-sprayed alloy and the as-cast alloy can be attributed to the high solidification rate occurring in the spray forming process, which is in the range of 10²–10³ K/s. With the increase of solidification rate, the nucleation rate of Si increases and the growth rate is suppressed. Thus, a large number of fine and uniformly distributed Si particles were formed in the as-spray formed Al–27% Si alloy.

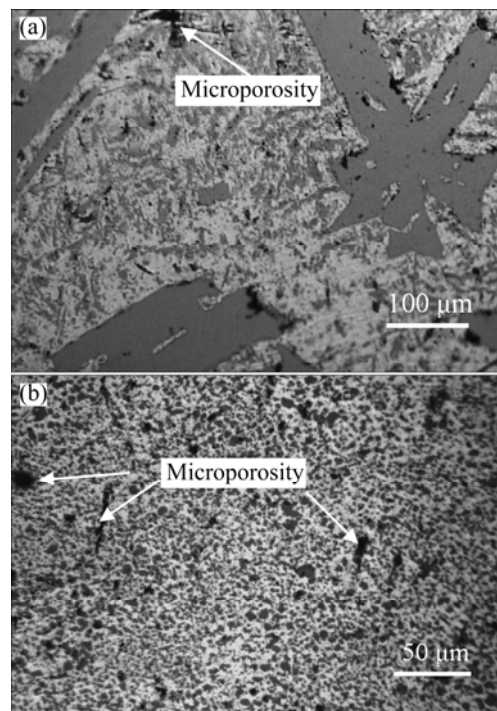


Fig. 2 Optical microstructures of Al–27%Si alloy: (a) As-cast; (b) As-sprayed

Figure 3 shows the microstructures of spray-formed Al–27%Si alloy reheated at 600 °C for various holding time. It is obvious that the primary Si is coarsening compared with the as-spray formed alloy, but the quantity of primary Si is reduced during the reheating process. As shown in Figs. 3(a) and (b), after reheating at 600 °C for 4–8 min, there is no liquid phase in the specimens. The primary Si at grain boundary grows up

and the fine primary Si in the matrix disappears. It can be regarded as a solid phase transformation process. Gibbs–Thomson effect shows that the small precipitation particles in the solid solution have high interface energies. This means that the small particle is unstable and has a trend to disappear. On the contrary, the big precipitation particles have low interface energies and they are easy to grow up. In this work, the primary Si is

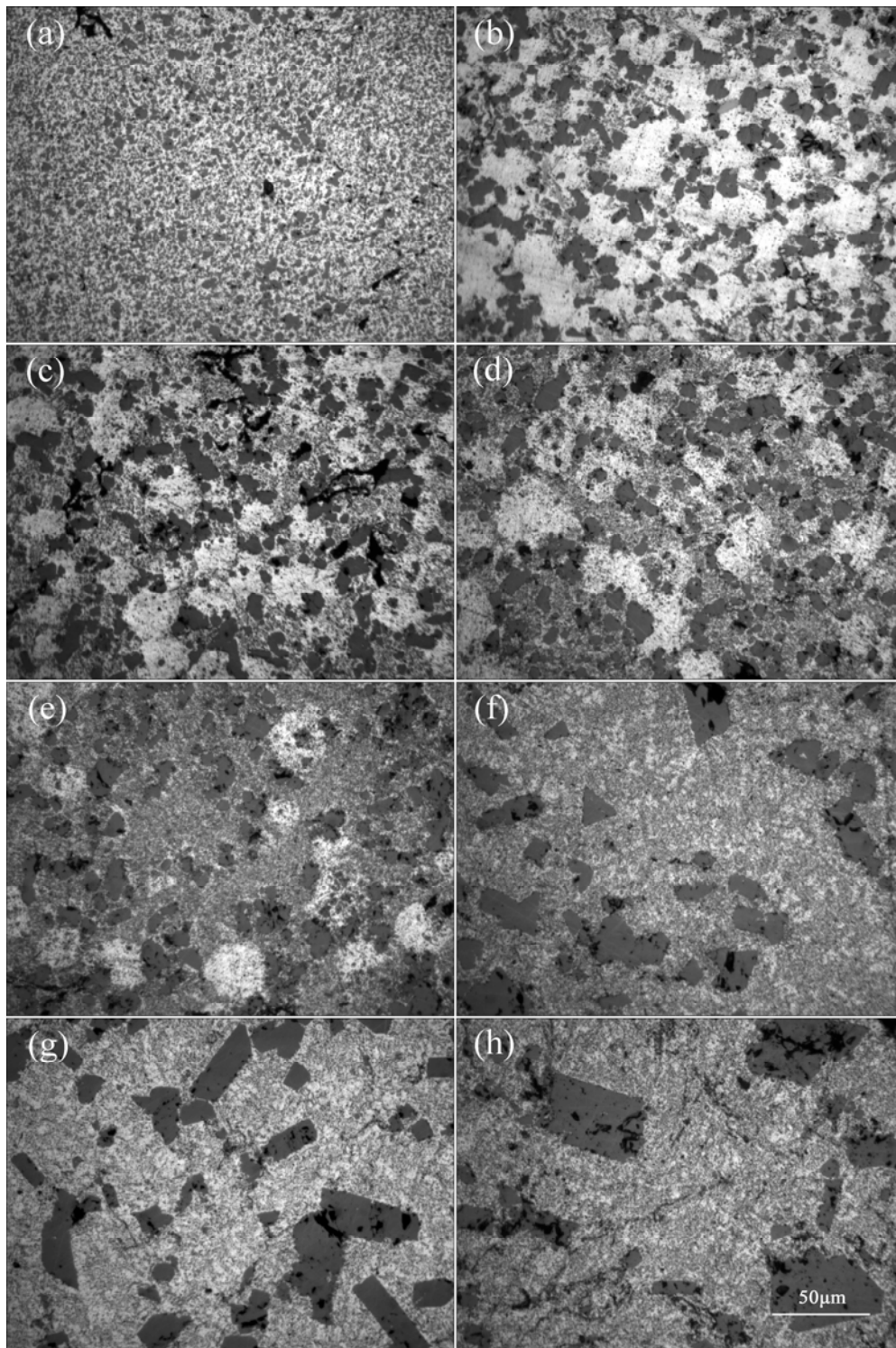


Fig. 3 Optical microstructures of spray-formed Al–27%Si alloy reheated at 600 °C for different time: (a) 4 min; (b) 8 min; (c) 10 min; (d) 12 min; (e) 14 min; (f) 16 min; (g) 30 min; (h) 60 min

regarded as a precipitation particle. Figure 3 (c) shows the microstructure of specimen reheated at 600 °C for 10 min. There is something difference from that of the specimen reheated for 8 min, namely, some light gray regions appear. The EDX analysis reveals that the light gray region is eutectic Al–Si phase. It can be inferred that this region is liquid phase during the reheating process. The light gray region increases with the reheating time extension as shown in Figs. 3(d) and (e). This means that the liquid phase increases. Figure 3 (f) shows that the whole $\alpha(\text{Al})$ matrix becomes liquid phase. According to results by DU et al [15], the diffusion coefficient of Si in liquid Al is 3 orders of magnitude larger than that of Si in solid Al. Furthermore, the diffusion rate of Si in liquid phase is enhanced due to the liquid phase convection, and the primary Si coarsens rapidly, as shown in Figs. 3(g) and (h).

Figure 4 shows the SEM images of the spray-formed Al–27%Si alloy reheated at 600 °C for 12 min and deeply etched with 20% NaOH solution. Spray-formed billet is accumulated by tiny semisolid droplets, which are atomized by atomization gas. The interface between different droplets always has pore, vacancy, and impurity element. Si has a trend to precipitate, aggregate and grow at this high energy state interface. This phenomenon can be demonstrated by SEM images, as shown in Fig. 4. The primary Si and eutectic phase are around the $\alpha(\text{Al})$ matrix. SUN et al [16] found that the eutectic reaction starts with the Al-rich

spikes nucleation on the primary Al dendrites. The consequence of such morphological development is the formation of localized Si enrichment within interdendritic liquid and eventual segregation of numerous small silicon particles. Some of these small Si particles are then used as the nucleation sites for the eutectic Si.

3.2 Microstructure evolution hypothesis

Through detailed comparison and statistical analysis between the microstructure evolutions and the reheating process, the distinct microstructure evolution can be divided into three stages, as shown in Fig. 5.

As mentioned before, the first stage is a solid phase transformation process. The small particle tends to disappear and the large particle grows up. This phenomenon can be analyzed by the concentration difference of Si in solid solution at spray forming state and in the equilibrium $\alpha(\text{Al})$ matrix, and the interface energy difference between large and fine Si particles. Figure 6 shows the scheme of Si concentration distribution during the heat treatment, in which C_0 is the concentration of Si in $\alpha(\text{Al})$ solid solution during spray forming; C_α and C_β refer to the equilibrium concentrations of $\alpha(\text{Al})$ and primary Si, respectively. There is a concentration difference between C_0 and C_α ($C_0 - C_\alpha > 0$), where the concentration equilibrium is broken. Then the volume diffusion of solute Si in the $\alpha(\text{Al})$ matrix starts, the Si atoms diffuse from the high

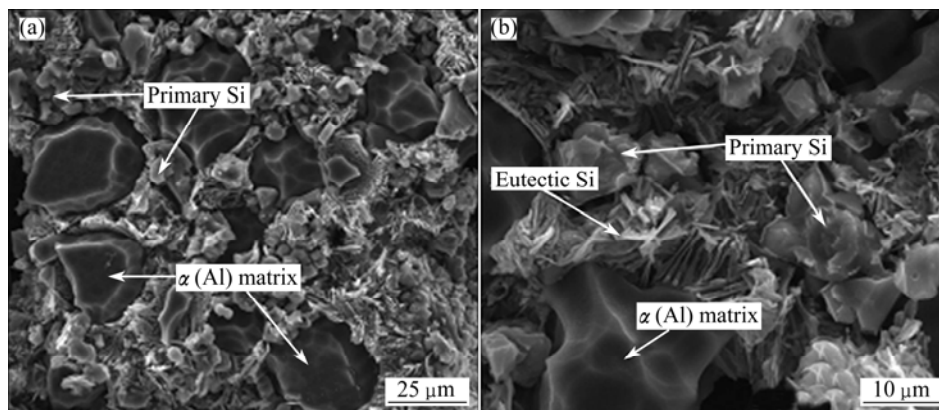


Fig. 4 SEM images of spray-formed Al–27%Si alloy reheated at 600 °C for 12 min (deeply etched)

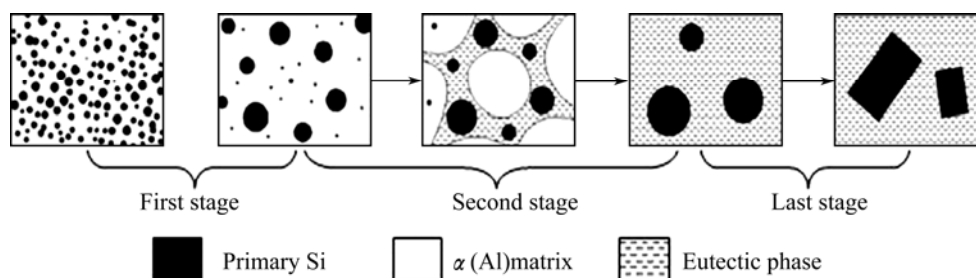


Fig. 5 Scheme of microstructure evolution of spray-formed Al–27%Si alloy in semisolid state

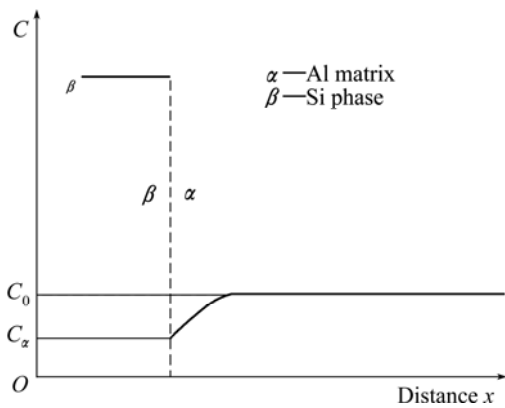


Fig. 6 Scheme of Si concentration distribution during heat treatment

concentrated $\alpha(\text{Al})$ phases into the low concentrated $\beta\text{-Si}$ phases. Figure 7 shows the relationship between free energy and the compositions in $\alpha(\text{Al})$ solid solution, such as large $\beta\text{-Si}$ particles and fine $\beta\text{-Si}$ ones. The fine $\beta\text{-Si}$ particles have a larger specific surface and a higher interface energy than the large ones ($r_1 > r_2, G_{\beta r_1} < G_{\beta r_2}$). According to common Tangent law, when the precipitated Si particle has a size of r_1 , the solid solubility of $\alpha(\text{Al})$ matrix is C_{r_1} , and when the precipitated Si particle has a size of r_2 , the solid solubility of $\alpha(\text{Al})$ matrix is C_{r_2} ($C_{r_1} < C_{r_2}$). There is a concentration difference between different sizes Si particles and $\alpha(\text{Al})$ matrix. The atoms of fine $\beta\text{-Si}$ particles start to diffuse and precipitate around the large $\beta\text{-Si}$ particles. This phenomenon results in the dissolving and disappearing of fine Si particles, the coarsening of large $\beta\text{-Si}$ particles and the decreasing of quantity of Si particles.

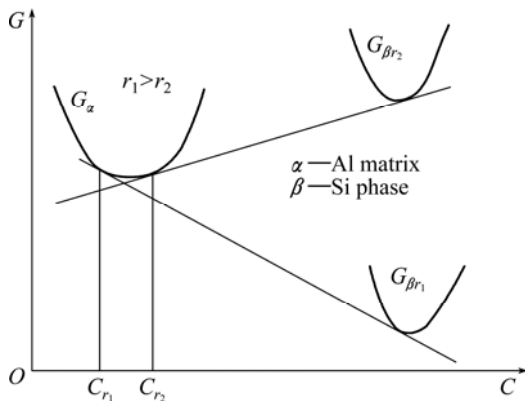


Fig. 7 Relationship between free energy and composition in $\alpha(\text{Al})$ solid solution including large $\beta\text{-Si}$ particles and fine $\beta\text{-Si}$ ones

At the second stage, the region around the $\alpha(\text{Al})$ matrix gradually melts. The primary Si in the liquid phase grows up obviously. However, in the solid phase,

the quantity of primary Si is reduced obviously. At last, eutectic phase appears when the specimen is quenched in cold water. The last stage is similar as the second stage except that all the $\alpha(\text{Al})$ matrixes are melted. At this stage, primary Si grows up rapidly.

The trend of microstructure evolution in semisolid state is similar at different reheating temperatures. But, the coarsening rate of the primary Si is accelerated at high reheating temperatures and the three stages become much shorter than at low temperatures. Figure 8 shows the liquid volume fraction of spray-formed Al–27% Si alloy reheated for different time in semisolid state at various temperatures, which was analyzed by the metallurgical analysis software using the fractal description method. The holding time for reaching the solid–liquid equilibrium at 590 °C is about 30 min, while it is only 10 min when reheated at 610 °C. In this work, the microstructure evolution of Al–27% Si alloy reheated at 600 °C was analyzed and discussed as an example. It is easier to find that the microstructure evolution is distinct in any stage.

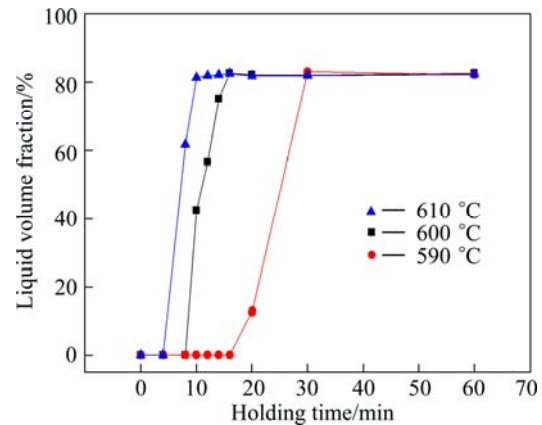


Fig. 8 Liquid volume fraction vs holding time at various temperatures for spray-formed Al–27% Si alloy

The typical theory was developed by LIFSHITZ, SLYOZOV and WAGNER (LSW theory) [17], in which the relationship among the mean particle size, temperature and holding time is as follows:

$$K_{\text{LSW}}t = \frac{8}{9} \frac{D\sigma\Omega C_{\infty}}{k_{\beta}\theta(C_{\beta} - C_{\infty})} t \tag{1}$$

where K_{LSW} is the coarsening rate constant; θ and t represent the temperature and the holding time, respectively; D is the diffusivity of solute in the matrix; σ is the surface energy; Ω is the atomic volume; k_{β} is Boltzman constant; C_{β} and C_{∞} are the equilibrium concentration of solute in the coarsening phase and in the matrix, respectively. This means that the size of the coarsening phase is controlled by the coarsening rate K_{LSW} and the holding time t . K_{LSW} is calculated for two parts in the case of solid state and liquid state. Table 1

lists the coarsening rates K_{LSW} in liquid and solid phase at different temperatures using the data listed in Table 2. The coarsening rate K_{LSW} is $3\text{--}4\ \mu\text{m}^3/\text{s}$ in liquid phase, but only $0.2\text{--}0.3\ \mu\text{m}^3/\text{s}$ in the solid phase. This is the reason why the coarsening of primary Si in the first stage is not obvious, but quite rapidly in the last two stages. The coarsening rate K_{LSW} increases with the increase of the reheating temperature both in the liquid and solid phases.

Table 1 Coarsening rates K_{LSW} in liquid and solid phases at different temperatures

$\theta/^\circ\text{C}$	$K_{LSW}/(\mu\text{m}^3\cdot\text{s}^{-1})$	
	Liquid phase	Solid phase
590	3.52	0.18
600	3.87	0.23
610	4.16	0.29

Table 2 Materials parameters used for calculation about Al–27%Si alloy [15,18]

Element	In liquid Al	In FCC Al	Relative atomic mass	Density/ ($\text{g}\cdot\text{cm}^{-3}$)	Molar volume/ ($\text{m}^3\cdot\text{mol}^{-1}$)	Surface energy, $\sigma/(\text{J}\cdot\text{cm}^{-2})$	w/%
Si	$D_0=1.34\times 10^{-7}\ \text{m}^2/\text{s},$ $Q=30\ \text{kJ/mol}$	$D_0=1.38\times 10^{-5}\ \text{m}^2/\text{s},$ $Q=117.6\ \text{kJ/mol}$	28.08	2.329	1.05×10^{-5}	0.8248	27
Al			26.98	2.698			73

$$D=D_0\exp[-Q/(RT)]$$

For better characterization of the microstructure evolution in the above three stage, spray-formed Al–27%Si alloys were reheated at $600\ ^\circ\text{C}$ for 4, 8, 12, 60 min and the specimens were deeply etched with 20% NaOH solution. In the first stage, as shown in Figs. 9(a) and (b), primary Si grows up around $\alpha(\text{Al})$ matrix. Figure 9(c) represents the second stage, namely eutectic Si appears in the melted region. Figure 9(d) represents the last stage, namely primary Si continues growing up to be plate-like and eutectic Si appears in the matrix. This microstructure evolution procedure is identical with the scheme mentioned above.

4 Conclusions

1) The spray forming process exhibits considerable microstructure refinements in Al–27%Si alloy. The fine primary Si is uniformly distributed in the $\alpha(\text{Al})$ matrix.

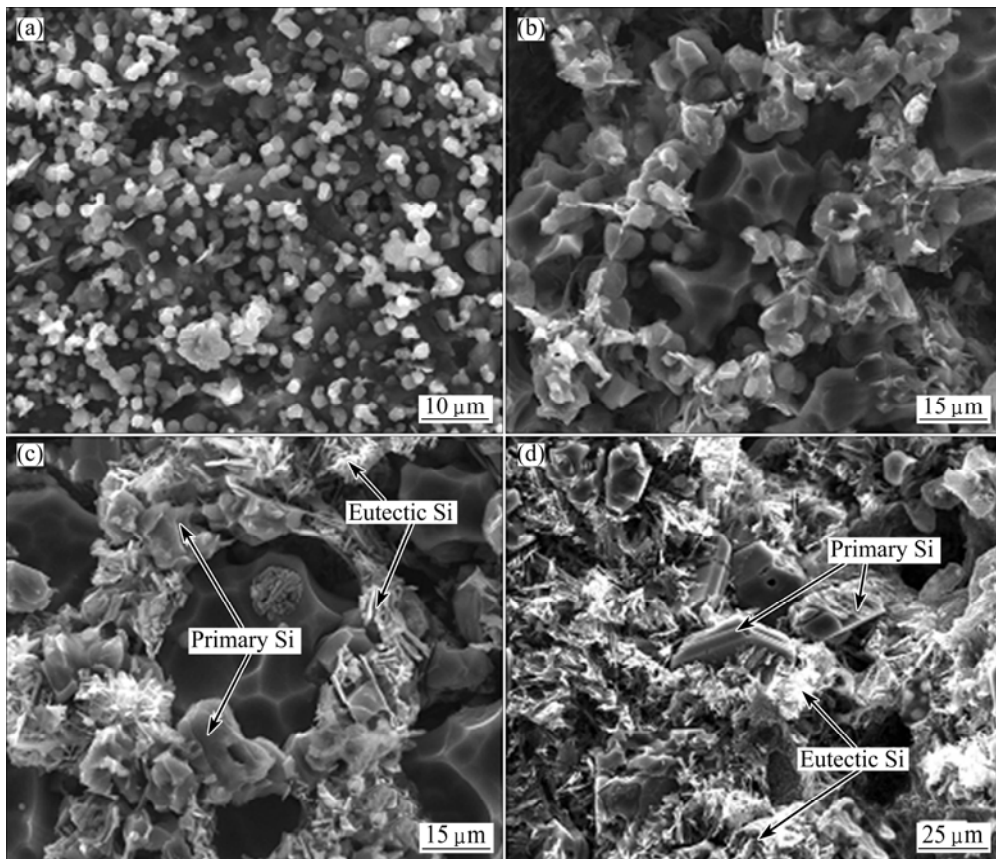


Fig. 9 SEM images of spray-deposited Al–27%Si alloy reheated at $600\ ^\circ\text{C}$ for different holding time (deeply etched): (a) 4 min; (b) 8 min; (c) 12 min; (d) 60 min

2) The microstructure evolution in the semisolid state can be divided into three stages. The first stage is a solid phase transformation process with the characteristics of the primary Si phase coarsening and the quantity of primary Si decreasing. In the second stage, the region around the $\alpha(\text{Al})$ matrix gradually melts. The primary Si in the liquid phase grows up obviously. Eutectic phase is produced in the molten region when the specimens are quenched in cold water. The last stage is similar as the second stage except that all the $\alpha(\text{Al})$ matrixes are melted.

3) The coarsening rates of the primary Si reheated at 590, 600 and 610 °C are calculated to be 3–4 $\mu\text{m}^3/\text{s}$ in the liquid phase, but just 0.2–0.3 $\mu\text{m}^3/\text{s}$ in the solid phase. The coarsening rate increases with the increase of reheating temperature both in the liquid and solid phases.

References

- [1] YU K, LI C, YANG J, CAI Z Y. Production and properties of a 90%Si–Al alloy for electronic packaging applications [J]. Materials Science Forum, 2009, 610–613(1): 542–545.
- [2] XIU Z Y, GAO G Q, YANG W S, SONG M H, WU G H. Microstructure and thermal properties of recyclable Sip/1199Al composites [J]. Transactions of Nonferrous Metals Society of China, 2009, 19(6): 1440–1443.
- [3] SRIVASTAVA V C, MANDAL R K, OJHA S N. Microstructure and mechanical properties of Al–Si alloys produced by spray forming process [J]. Materials Science and Engineering A, 2001, 304–306: 555–558.
- [4] FERRARINI C F, BOLFARINI C, KIMINAMI C S, BOTTA W J F. Microstructure and mechanical properties of spray deposited hypoeutectic Al–Si alloy [J]. Materials Science and Engineering A, 2004, 375–377: 577–580.
- [5] SRIVASTAVA V C, GHOSAL P, OJHA S N. Microstructure and phase formation in spray-deposited Al–18%Si–5%Fe–1.5%Cu alloy [J]. Materials Letters, 2002, 56: 797–801.
- [6] CUI C, SCHULZ A, SCHIMANSKI K, ZOCH H W. Spray forming of hypereutectic Al–Si alloys [J]. Journal of Materials Processing Technology, 2009, 209: 5220–5228.
- [7] BERETA L A, FERRARINI C F, KIMINAMI C S, BOTTA W J F, BOLFARINI C. Microstructure and mechanical properties of spray deposited and extruded/heat treated hypoeutectic Al–Si alloy [J]. Materials Science and Engineering A, 2007, 449–451: 850–853.
- [8] SEOK H K, LEE J C, LEE H I. Extrusion of spray-formed Al–25Si–X composites and their evaluation [J]. Journal of Materials Processing Technology, 2005, 160: 354–360.
- [9] WOLFSDORF T L, BENDER W H, VOORHEES P W. The morphology of high volume fraction solid-liquid mixtures: An application of microstructure tomography [J]. Acta Materialia, 1997, 45(6): 2279–2295.
- [10] CHANG C P, CHI Y A, TSAO. Workability of spray-formed Al/SiP metal matrix composites [J]. Key Engineering Materials, 2003, 249: 189–194.
- [11] CAO Fu-rong, GUAN Ren-guo, CHEN Li-qing, ZHAO Zhan-yong, REN Yong. Microstructure evolution of semisolid AZ31 magnesium alloy during reheating process [J]. The Chinese Journal of Nonferrous Metals, 2012, 22(1): 7–14. (in Chinese)
- [12] ZHANG D, YANG B, ZHAN J S, ZHANG Y A, XIONG B Q. Effect of deformation temperature and strain rate on semi-solid deformation behavior of spray-formed Al–70%Si alloys [J]. Transactions of Nonferrous Metals Society of China, 2005, 15(5): 1125–1129.
- [13] WARD P J, ATKINSON H V, ANDERSON P R G, ELIAS L G, GARCIA B, KAHLEN L, RODRIGUES-IBABE J M. Semi-solid processing of novel MMCs based on hypereutectic aluminum–silicon alloys [J]. Acta Materialia, 1996, 44(5): 1717–1727.
- [14] CHIANG C H, CHI Y A, TSAO. Si coarsening of spray-formed high loading hypereutectic Al–Si alloys in the semisolid state [J]. Materials Science and Engineering A, 2005, 396: 263–270.
- [15] DU Y, CHANG Y A, HUANG B Y, GONG W P, JIN Z P, XU H H, YUAN Z H, LIU Y, HE Y H, XIE F Y. Diffusion coefficients of some solutes in FCC and liquid Al: Critical evaluation and correlation [J]. Materials Science and Engineering A, 2003, 363: 140–151.
- [16] SUN Y, PANG S P, LIU X R, YANG Z R, SUN G X. Nucleation and growth of eutectic cell in hypoeutectic Al–Si alloy [J]. Transactions of Nonferrous Metals Society of China, 2011, 21(10): 2186–2191.
- [17] HARDY S C, VOORHEES P W. Ostwald ripening in a system with a high volume fraction of coarsening phase [J]. Metallurgical Transactions A, 1988, 19: 2713–2721.
- [18] GOICOECHEA J, GARCIA-COROVILLA C, LOUIS E, PAMIES A. Surface tension of binary and ternary aluminum alloys of the systems Al–Si–Mg and Al–Zn–Mg [J]. Journal of Materials Science, 1992, 27: 5247–5252.

半固态二次加热过程中喷射沉积过共晶 Al–Si 合金的显微组织演变

朱学卫, 王日初, 彭建, 彭超群

中南大学 材料科学与工程学院, 长沙 410083

摘要: 采用喷射沉积技术制备 Al–27%Si 合金, 研究半固态二次加热过程中该合金显微组织的演变。结果表明, 初晶硅在二次加热过程中发生粗化, 并且粗化速率随着二次加热温度的升高而增大, 液态区域凝固后出现共晶组织。在二次加热过程中喷射沉积过共晶 Al–Si 合金的显微组织演变可以分为 3 个阶段: 第一阶段属于固态相转变; 在第二阶段 Al 基体周围开始逐渐熔化, 熔化区域内初晶硅粗化明显且经水淬后出现共晶组织; 第三阶段与第二阶段类似, Al 基体熔化。

关键词: 喷射沉积; Al–Si 合金; 半固态; 粗化率